

LOCALIZED POLARIZATION BEHAVIOR AND INFERRED GRAIN SIZE DISTRIBUTION AT THE LUNAR SWIRL REINER GAMMA IN COMPARISON TO CRATER RAYS AND EJECTA BLANKETS.

C. Wöhler¹, M. Bhatt², M. Arnaut¹, ¹Image Analysis Group, TU Dortmund University, 44227 Dortmund, Germany, christian.woehler@tu-dortmund.de, ²Physical Research Laboratory, Ahmedabad, 380009, India, megha@prl.res.in.

Introduction: The linear polarization state of the light reflected from the lunar surface is an indicator of the small-scale structure of the regolith, in particular its grain size and microscopic roughness [1, 2]. In this work we present new high-resolution telescopic imaging polarization data of localized areas in western Oceanus Procellarum, focusing on the polarization behavior of the swirl structure Reiner Gamma in comparison to surrounding crater rays and ejecta blankets in order to better understand the formation of the swirl.

Data and Methods: The imaging polarization data analyzed in this work were acquired with a monochrome industrial polarization camera The Imaging Source DZK 33GX250, whose individual sensor pixels are equipped with polarization filters rotated by 0°, 45°, 90° and 135° [3]. This camera was attached to a Newton reflector telescope of 200 mm diameter. The primary focal length of 1.2 m was extended to 3.0 m using a Barlow lens, leading to a resolution of 0.9 km per pixel of the polarization image.

In this configuration, a set of 3500 frames was acquired in the Johnson R band on December 16th, 2022, at a phase angle of 87.5°. From each frame the individual sub-frames corresponding to the four polarization directions were extracted, and the sharpest 10% of the sub-frames of each polarization direction were selected and stacked with the software Autostakkert3 [4]. From the resulting 32-bit image data we inferred the pixel-wise intensity F (Fig. 1), fraction P of linearly polarized light, and angular direction W of linear polarization (Fig. 2).

To estimate the regolith grain size, we used the method of [1], which relies on a fit of the relation $b = a \log P + \log A$ to all pixels, where A is the albedo. For small surface areas with negligible variations in illumination and observation geometry, the pixel intensity F can be assumed to be proportional to the albedo A . We thus replaced A by F and shifted the points in the $(\log P, \log F)$ diagram horizontally such that the resulting value of b corresponds, according to eq. 10 of [1], to the average grain size of mature mare regolith of 47 μm [2]. In this way, the grain size d can be computed for each pixel based on the corresponding values of F and P . Each of our studied surface areas has a size of 251 by 251 pixels.

Results: As shown in Fig. 2, the grain size exhibits strong variations across Reiner Gamma in the main oval, the northeastern tail and the southwestern small

structures. Apparent grain size variations inside the craters Reiner, Kepler and Aristarchus are presumably artifacts due to topography-dependent surface illumination. The reduced grain size at the volcanic plateau northwest of Aristarchus has already been described in [1]. For the bright rays around Kepler and Aristarchus and south of Seleucus, the grain size variations are weaker than at Reiner Gamma or absent. Only ejecta blankets of small craters near Reiner, Kepler and in the mare near Seleucus show grain size anomalies similar in strength to those observed at Reiner Gamma. Furthermore, most parts of Reiner Gamma, the ray system of Kepler, the Seleucus ray and the bright area around Aristarchus show distinct anomalies of the angular polarization direction, whose origins remain to be explained.

Discussion: The variable strength of the grain size variations at crater rays and ejecta blankets despite similar variations in brightness (which are caused by maturity and/or composition [5]) are presumably due to differences in age and thus space-weathering state. The grain size variations across Reiner Gamma need to be explained by a mechanism that goes beyond magnetic shielding [6], i.e., by an external mechanism such as the interaction between the regolith and the gaseous hull of a passing comet (e.g., [7]) that separated different grain size fractions on kilometer scales.

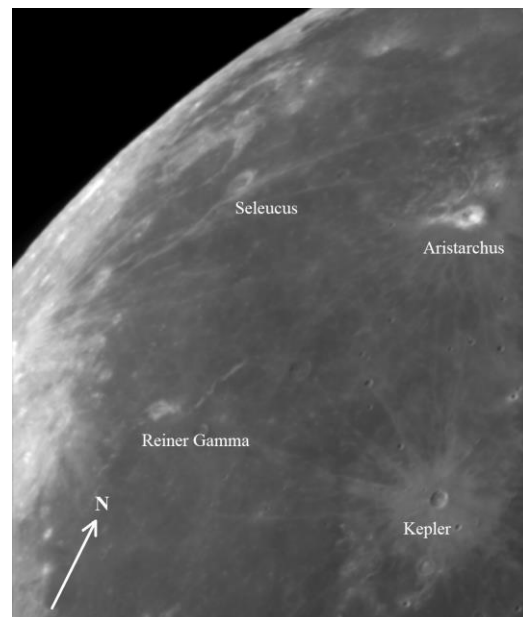


Figure 1: Intensity image of western Oceanus Procellarum.

References: [1] Shkuratov, Y. and Opanasenko, N. (1992) *Icarus* 99(2), 468-484. [2] Dollfus, A. (1998) *Icarus* 136(1), 69-103. [3] The Imaging Source (2019) [https://www.theimagingsource.com/products/industrial-cameras/gige-](https://www.theimagingsource.com/products/industrial-cameras/gige-polarsens/dzk33gx250/)

[polarsens/dzk33gx250/](https://www.theimagingsource.com/products/industrial-cameras/gige-polarsens/dzk33gx250/) [4] Kraaikamp, E. (2023) <https://www.autostakkert.com> [5] Hawke, B. R. et al. (2004) *Icarus* 170(1), 1-16. [6] Glotch, T. et al. (2015) *Nature Comm.* 6, 6189. [7] Hess, M. et al. (2020) *A&A* 639, A12.

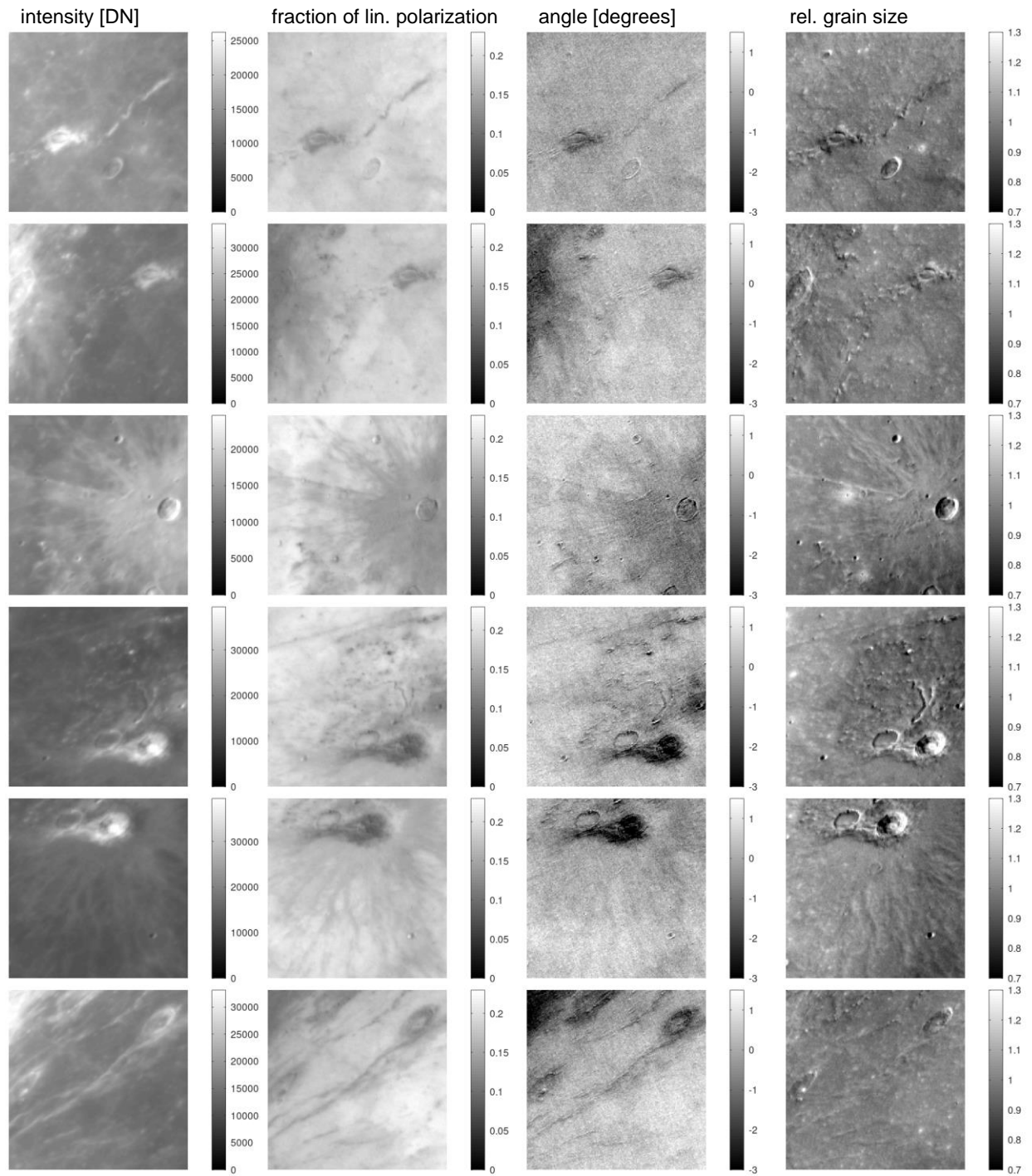


Figure 2: Regional polarization data. From left to right: Intensity (in DN), fraction of linear polarization, angle of the polarization plane (degrees, relative to mean angle), and grain size (relative to the assumed average mare value of 47 μm). From top to bottom: Reiner Gamma northeast and southwest, Kepler, Aristarchus volcanic plateau and southern rays, Seleucus ray.